Thermodynamic nature of and spontaneous strain below the cubic–monoclinic phase transition in $La_2Mo_2O_9$

2004 J. Phys.: Condens. Matter 16 3571

(http://iopscience.iop.org/0953-8984/16/21/007)

INSTITUTE OF PHYSICS PUBLISHING JOURNAL OF PHYSICS: CONDENSED MATTER

J. Phys.: Condens. Matter **16** (2004) 3571–3583 PII: S0953-8984(04)62912-2

Thermodynamic nature of and spontaneous strain below the cubic–monoclinic phase transition in $La_2Mo_2O_9$

Stuart A Hayward and Simon A T Redfern

Department of Earth Sciences, University of Cambridge, Downing Street, Cambridge CB2 3EQ, UK

Received 28 April 2003, in final form 29 March 2004
Published 14 May 2004
Online at stacks.iop.org/JPhysCM/16/3571
DOI: 10.1088/0953-8984/16/21/007

Abstract

The pseudocubic lattice parameter of lanthanum molybdate, $La_2Mo_2O_9$, has been measured as a function of temperature between 13 and 1100 K. These data show an anomaly at 842 K, associated with the alpha (pseudocubic monoclinic, non-conducting) to beta (cubic, conducting) phase transition. For a sample which has been quenched from high temperatures, the $a(T)$ data are continuous across this transition, indicating that the transition is smeared or thermodynamically second order. When the same material is cooled slowly, subsequent measurements show the transition to be first order, with a similar transition temperature. The difference between these two behaviours is attributed to changes in oxygen ordering resulting from different thermal histories.

1. Introduction

Oxide ion conductors have a wide range of potential applications, including as the electrolyte in solid-oxide fuel cells, as oxygen sensors and acting as an oxygen-permeable membrane in catalytic systems. Although research into fast oxide conductors can be traced back to the study of fluorine ion conduction in lead fluoride by Faraday (1839), commercial application of these materials has always been hampered by the high temperatures needed for useful conductivity.

Whilst oxide ion conductors based on stabilized zirconia have good conductivity above about 1000 °C, the use of oxide ion conductors in fuel cells requires conductivity at significantly lower temperatures, with 600–700 °C often quoted as a target temperature. In the fluorite/zirconia structure type, conductivity is enhanced by increasing the concentration of vacancies extrinsically, by replacing some high valency cations (such as Zr^{4+} in zirconia) with lower valency cations (such as Y^{3+} or Ca^{2+}), compensated by vacancies on the oxygen sites.

An alternative strategy is to use a material with more anion sites than there are anions to fill them. The unoccupied sites—intrinsic vacancies—may outnumber the occupied anion

sites, which will greatly enhance the anion mobility. In such materials, there is often a phase transition between a high temperature phase with anions disordered over many equivalent sites and a low temperature phase where the occupied and unoccupied sites form two separate sublattices. In such cases, there will be a large increase in the conductivity of the material at the phase transition.

Lanthanum molybdate has been proposed (Goutenoire *et al* 2000, Lacorre *et al* 2000) as a promising oxide ion conductor of the intrinsic vacancy type. Its conductivity at 800 °C is 0.08 S cm^{-1} (Goutenoire *et al* 2001), which is comparable with those for the typical stabilized zirconia materials. The conductivity falls with reducing temperature, according to usual thermal activation behaviour, and also has a rather abrupt reduction of two orders of magnitude at the order–disorder phase transition ($T_C = 580$ °C). Crucially, this transition temperature is less than the 600–700 °C limit below which the engineering difficulties associated with oxide ion conductors become less difficult to overcome. Thus, this structural family was heralded as a structural paradigm alternative to the traditional solid electrolyte oxides such as perovskite, fluorite and pyrochlore. Substitutions on both the La and Mo sites have been examined in an attempt to further enhance the properties of lanthanum molybdate (Goutenoire *et al* 2000, Collado *et al* 2002, Wang and Fang 2002, Wang *et al* 2002, Georges *et al* 2003).

Since the initial observation that lanthanum molybdate is a promising oxide ion conductor, a number of studies have examined various aspects of the behaviour of $La_2Mo_2O_9$, with the phase transition as one of the key points of interest. Despite this, the ordered room temperature structure of $La_2Mo_2O_9$ is, as yet, unsolved. One reason for this is that the low temperature structure appears to be only very slightly distorted from the high temperature cubic phase, which has space group $P2_13$. The second difficulty is that the unit cell of the ordered structure is 24 times larger than that of the disordered structure. Although the unit cell of ordered $La_2Mo_2O_9$ contains too many atoms to allow its structure to be determined reliably, the structure of the disordered phase, shown in figure 1, was determined using x-ray and neutron powder diffraction (Goutenoire *et al* 2001), and solved on the basis of its similarity to that of β-$SnWO_4$. This structure was slightly readjusted by Lacorre *et al* (2003). It is known that of the three distinct oxygen ion sites in the cubic structure, only one (described as O1 in the structure of Goutenoire *et al* 2001) is completely occupied. The other two site types have occupancies of around 2/3 for the O2 site and 1/3 for the O3 site. On average, La is coordinated by nine oxygen atoms distributed over 15 possible sites, and Mo is coordinated by four oxygen atoms on seven sites.

The symmetry breaking spontaneous strains associated with the cubic—monoclinic phase transition are extremely small, though they can be measured in very high resolution experiments; Georges *et al* (2003) found the monoclinic cell angle $\beta = 89.6°$ at room temperature. The non-symmetry breaking strain is larger and more easily measured. Differential thermal analysis shows anomalies associated with the phase transition. For fast heating and cooling rates, the anomaly is peak shaped with large hysteresis. The magnitudes of both the peak and the hysteresis increase with increasing temperature ramp rates, as found by Wang and Fang (2001). These workers also studied the nature of the dielectric and anelastic loss in $La_2Mo_2O_9$, which they were able to relate to oxygen ion hopping between the three types of oxygen site. These thermal analysis data and the spontaneous strain data have been interpreted as evidence that the transition is thermodynamically first order.

To better characterize this phase transition, we have studied the structure of $La_2Mo_2O_9$ by means of x-ray powder diffraction as a function of temperature, extending the range of temperatures studied to both higher and lower temperatures than in previous experiments. The evolution of the structure at high temperatures is significant, since this is the operating range for any device using $La_2Mo_2O_9$ as a conducting material. Data recorded above the transition temperature

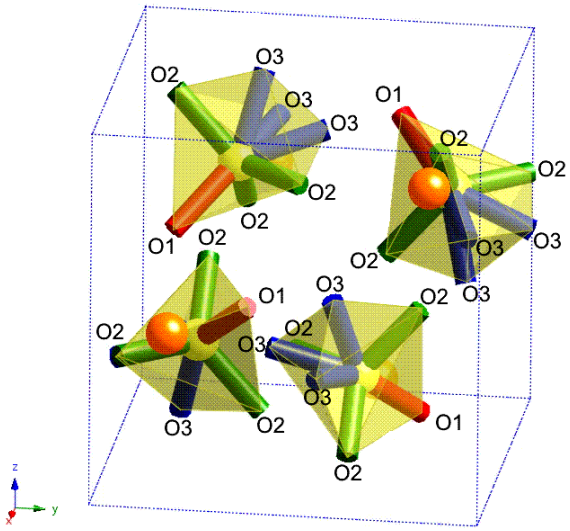

Figure 1. The cubic ($P2_13$) structure of $La_2Mo_2O_9$ (data from Goutenoire *et al* 2001), with the unit cell indicated. The large spheres represent La; the polyhedra are centred on Mo, with O sites at their vertices. The red bonds within these polyhedra are to the fully occupied O1 sites, and the green and blue bonds are to the partially occupied O2 and O3 sites respectively.

(This figure is in colour only in the electronic version)

also allow the baseline behaviour of the paraphase to be constrained, which is essential for the proper calculation of the spontaneous strain below T_C (Carpenter *et al* 1998). We also find that the behaviour of the low temperature structure is sensitive to the thermal history of the material.

2. Experimental methods

2.1. Sample synthesis and characterization

Sintered polycrystalline ceramic pellets of $La_2Mo_2O_9$ were prepared following conventional solid-state reaction methods. A stoichiometric mixture of 99.999% La_2O_3 and MoO_3 reagents was thoroughly ground and mixed by hand in an agate mortar under acetone. These mixtures were then calcined at 1 atm in a box furnace at 1073 K for 16 h, before being cold pressed and subsequently sintered at 1223 K for 44 h in air and then quenched in air to room temperature. This produced dense homogeneous ceramic pellets, 13 mm in diameter, which were used for subsequent study.

The sample was initially characterized by means of ambient temperature x-ray powder diffraction using a Siemens D5000 instrument, which showed it to be single-phase $La_2Mo_2O_9$ with a pseudocubic unit cell similar to that previously reported. The sample was subsequently characterized by Raman and infrared spectroscopy. The Raman spectrum of our sample was collected in a 180° scattering geometry using a Jobin-Yvon LabRam 300 instrument, equipped with a ×50 microscope objective and a 632.817 nm laser. Powder infrared spectra were collected from samples diluted in KBr pellets (to obtain the mid-infrared spectrum) and polyethylene pellets (for the far infrared) using a Bruker 113 V instrument.

2.2. X-ray diffraction

X-ray power diffraction patterns were collected using two diffractometers optimized for the rapid and precise determination of lattice parameters at high and low temperatures. The basic

design is described in Salje *et al* (1993). For the current experiment, the apparatus was further enhanced by the use of a high intensity microsource x-ray generator (Bede Scientific), rather than a conventional x-ray tube. Cu Kβ radiation was used, in order to avoid the problem of resolving the Kα_1:Kα_2 doublet.

A diffractometer with a resistive Pt strip sample heater allowed powder diffraction spectra to be recorded at room temperature and in the temperature range 373–1100 K. A similar system fitted with a He cryostat permitted measurements between room temperature and 13 K.

Two distinct series of diffraction experiments were performed. In one sequence, the sample was mixed with silicon as an internal 2θ standard. This was not ideal, due to the closeness of the sample peaks at approximately 42.7° and 50.2° to the silicon peaks near 42.5° and 50.3°. Particular care had to be taken in the calibration process to ensure that these peaks were indexed consistently. A further potential difficulty is the risk that the sample will react chemically with the standard.

From room temperature, the sample/silicon mix held in the high temperature diffractometer was heated to 373 K, then in 50 K steps to 773 K, then in 10 K steps to 973 K and 20 K steps to 1093 K. The sample/silicon mix measured in the low temperature diffractometer was cooled from room temperature in 10 K steps to 13 K. In both cases, the counting time for each diffraction pattern was 2 h.

Because of the potential ambiguities in the calibrated diffraction experiments noted above, additional sequences of measurements were performed using a pure $La_2Mo_2O_9$ sample. From room temperature, the sample was heated to 373 K, then in 50 K steps to 1173 K. The sample was then cooled in 50 K steps back to room temperature, and then the whole heating and cooling sequence was repeated.

3. Data analysis and results

3.1. Calibrated measurements on a quenched sample: lattice parameter and transition temperature

The low temperature form of $La_2Mo_2O_9$ is monoclinic (Goutenoire *et al* 2000), but the deviations from cubic symmetry are extremely small. In the present experiment, it was not possible to measure any splitting of diffraction peaks reliably enough to calculate a symmetry breaking spontaneous strain. Some peak broadening was observed, but even this was difficult to study systematically. The additional diffraction maxima associated with the proposed $2a \times 3a \times 4a$ supercell of the monoclinic structure were too weak to detect. For these reasons, the lattice parameter of $La_2Mo_2O_9$ was determined on the basis of the high temperature pseudocubic unit cell ($a \approx 7.2$ Å) at all temperatures. The resulting $a(T)$ data are shown in figures 2 and 3. The transition is observed to occur at 842 ± 5 K. The first-order monoclinic–cubic transition temperature found by Goutenoire *et al* (2000) was about 580 °C, or 853 K. From internal friction measurements, Wang and Fang (2001) determined the transition temperature to be 833 K.

The lattice parameter data in the immediate vicinity of T_C show no evidence of a step change, implying that the transition in the sample studied in this experiment is thermodynamically second order (see, for example, Carpenter *et al* 1998), or that the transition is smeared by the interaction between the transition and an inhomogeneous conjugate field, possibly resulting from defect interactions. The lattice parameter of the cubic phase between 850 and 1093 K is given by $a = 7.019 + 2.173 \times 10^{-4}T$, where T is in kelvins and a in ångströms. The equivalent volume thermal expansion coefficient is 9.3×10^{-5} K^{-1}.

To convert these data into a thermodynamically useful form, the spontaneous strain due to the phase transition can be determined. Although the full form of the spontaneous strain

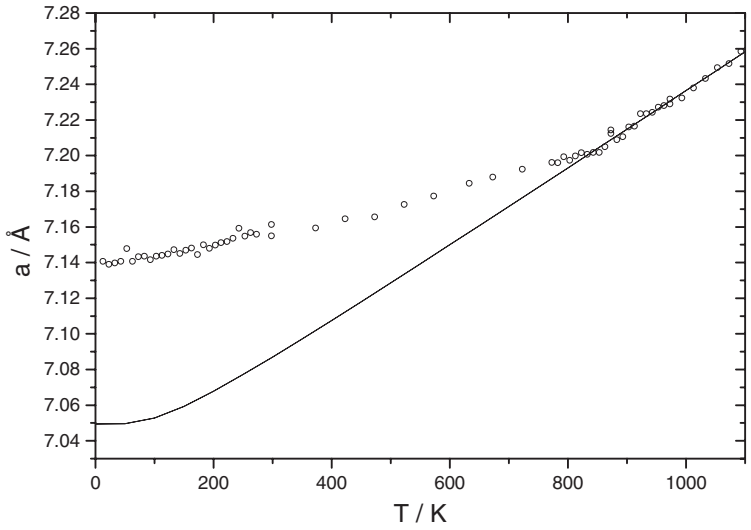

Figure 2. Variation of the pseudocubic lattice parameter for $La_2Mo_2O_9$ between 13 and 1093 K, showing the phase transition at 842 K. The solid curve shows the extrapolation of the high temperature baseline behaviour.

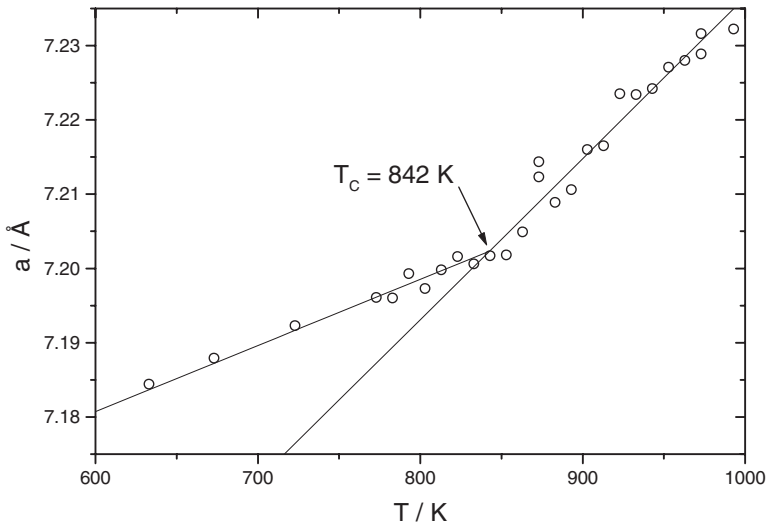

Figure 3. Enlargement of the $a(T)$ data for $La_2Mo_2O_9$ in the vicinity of the phase transition. The transition temperature is taken to be the temperature at which the $a(T)$ lines for the high and low temperature phases intersect.

is rather complex, having three degrees of symmetry breaking, the lack of observed peak splitting in the powder diffraction patterns means that the only strain measurable from these experimental data is the non-symmetry breaking volume strain, e_a. Describing both structures on the (pseudo)cubic axes, this strain is given by

$$e_a = 3e_1 = 3\left(\frac{a - a_0}{a_0}\right) = \left(\frac{V - V_0}{V_0}\right) \tag{1}$$

where a and V are the measured unit cell parameter volume at any given temperature, and a_0 and V_0 are the values which these parameters would have in the absence of the phase transition. The values of a_0 and V_0 are found by extrapolating the behaviour of a and V from above the transition, which requires a reasonably long run of data from above T_C (Carpenter *et al* 1998). Since the spontaneous strain e_a does not break the cubic symmetry of the high temperature phase, it is proportional to the square of the order parameter of the phase transition. The observation that e_a is proportional to $|T_C - T|$ implies that the thermodynamic behaviour of the transition is in the second-order limit (see, for example, section 4 of Carpenter *et al* 1998).

3.2. Fitting low temperature behaviour: the effect of quantum saturation

Whilst the a_0 baseline at moderately high temperatures is linear with temperature, the form of the baseline at lower temperatures requires more careful consideration. For reasons related to the vanishing of the specific heat as absolute zero temperature is approached, the thermal expansion coefficient of materials goes to zero at very low temperatures. In other words, the lattice parameter a and the extrapolated baseline lattice parameter a_0 tend to a constant. In the standard treatment of this problem (see, for example, Born and Huang 1954), the saturation of the thermal expansion occurs as the vibrational modes in a material are cooled into their ground state. Hayward *et al* (2002) use this argument to show that, using the Einstein model to approximate the phonon spectrum, the bare thermal expansion of a material is well approximated by

$$a(T) = a_0 + \frac{a_1\theta_E}{2}\coth\left(\frac{\theta_E}{2T}\right) \tag{2}$$

where θ_E is the Einstein temperature. At high temperatures ($T \gg \theta_E$), equation (2) simplifies to simple linear thermal expansion: $a(T) = a_0 + a_1T$.

Similarly, the order parameter of the phase transition (and hence the spontaneous strain) are required to saturate at low temperatures, as discussed by Pérez-Mato and Salje (2001). In the case of a second-order phase transition, the temperature dependence of the order parameter is given by

$$Q^2(T) = 1 - \frac{1}{T_C}\left(\theta_S\coth\left(\frac{\theta_S}{T}\right)\right) \tag{3}$$

as opposed to the classical model, $Q^2 = 1 - (T/T_C)$. In most cases, the value of the saturation temperature θ_S is dominated by the saturation of the soft mode associated with the phase transition. This in turn depends on the bare soft mode frequency, which is what the soft mode frequency would be in the absence of the phase transition.

Figure 2 shows that the thermal expansion of $La_2Mo_2O_9$ does saturate at low temperatures, but the observed saturation is a combination of two effects. Although θ_E could be calculated from very low temperature specific heat data, or estimated from the phonon density of states function, these data are currently unavailable for $La_2Mo_2O_9$. This is a problem, since the spontaneous strain data depend strongly on the choice of θ_E for the baseline, as shown in figure 4.

To give an objective criterion for the choice of θ_E, graphs of the spontaneous strain e_1 were plotted for a range of baselines, as shown in figure 4(a). The correct value of θ_E was taken to be that which caused the best-fit gradient of the e_1 versus T graph to go smoothly to zero at low temperatures, as predicted by equation (3). From these calculations, summarized in figures 4(b) and 5, the Einstein temperature of $La_2Mo_2O_9$ is estimated as 310 K and the saturation temperature for the order parameter is 165 K.

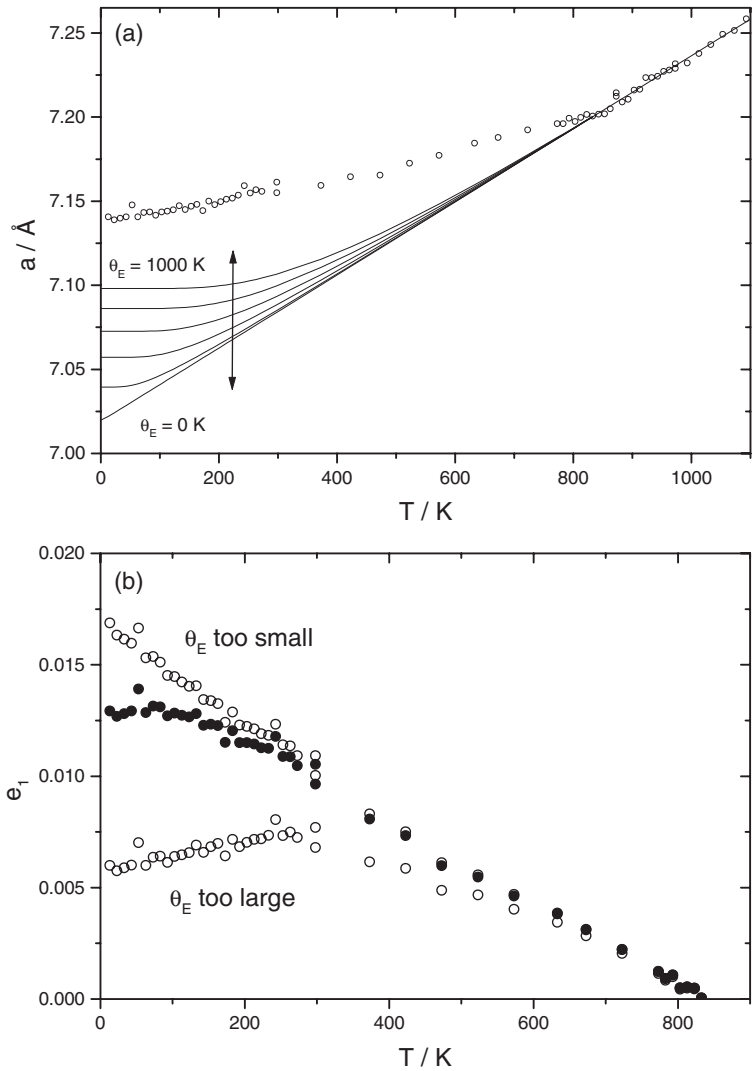

Figure 4. (a) Possible baseline thermal expansion curves, depending on the value of the Einstein temperature θ_E in $La_2Mo_2O_9$. (b) The effect of changing the Einstein temperature on the calculation of the spontaneous strain e_1. If θ_E is made too large (in this case 1000 K), the spontaneous strain falls on cooling, rather than just saturating. Similarly, if θ_E is made too small (in this graph, 0 K), the spontaneous strain continues to increase at low temperatures. For an appropriate value of θ_E ($\theta_E = 310$ K), the spontaneous strain tends to a constant as $T \rightarrow 0$ K (filled circles).

3.3. Kinetic effects from uncalibrated measurements

Whilst the use of an internal standard is generally advisable to obtain precise and reliable lattice parameters in an x-ray diffraction experiment, the use of a standard can lead to some difficulties. The most significant, particularly in high temperature experiments, is the possibility that the sample and standard will react. In order to remove this possibility, additional experiments were performed on the INEL diffractometer, using a pure $La_2Mo_2O_9$ sample mounted on the Pt–Rh heater strip. (The strip itself is not suitable for 2θ calibration, since it lies systematically

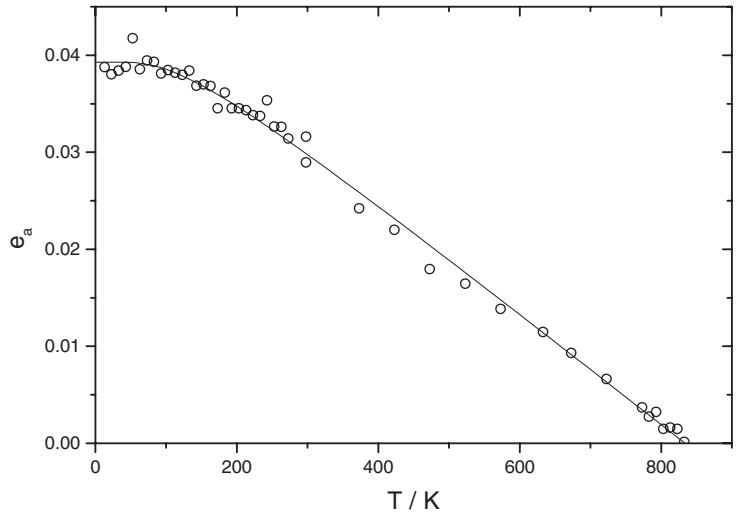

Figure 5. The temperature dependence of the non-symmetry breaking strain e_a, showing a fit to the quantum mechanical Landau model (equation (3) above). The fit parameters are $T_C = 833$ (6) K and $\theta_S = 165$ K.

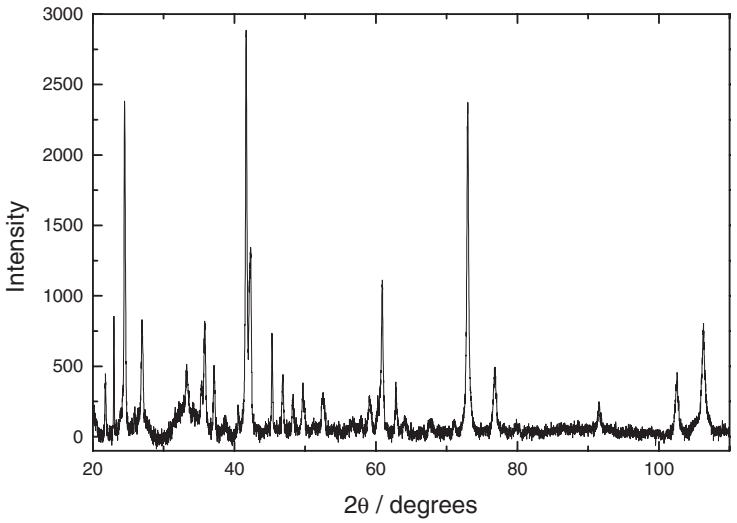

Figure 6. The diffraction pattern (with the background subtracted) of $La_2Mo_2O_9$ on a Pt–Rh strip at 723 K, collected without an internal Si standard.

below the sample in the diffractometer, and would therefore have a different position to 2θ calibration to the sample.) Comparison of the initial room temperature diffraction pattern with the equivalent Si-calibrated diffraction pattern allowed a 2θ scale to be determined. A typical spectrum is shown in figure 6.

To determine approximate lattice parameters from these spectra, the position of a single moderately high angle peak was followed as a function of temperature. The peak corresponding to (431) and (510) in the high temperature phase was used for this, since it is close to the (220) peak from the Pt–Rh strip, as shown in figure 7. This provided a qualitative check that the channel number to 2θ calibration function did not change excessively during the experiment.

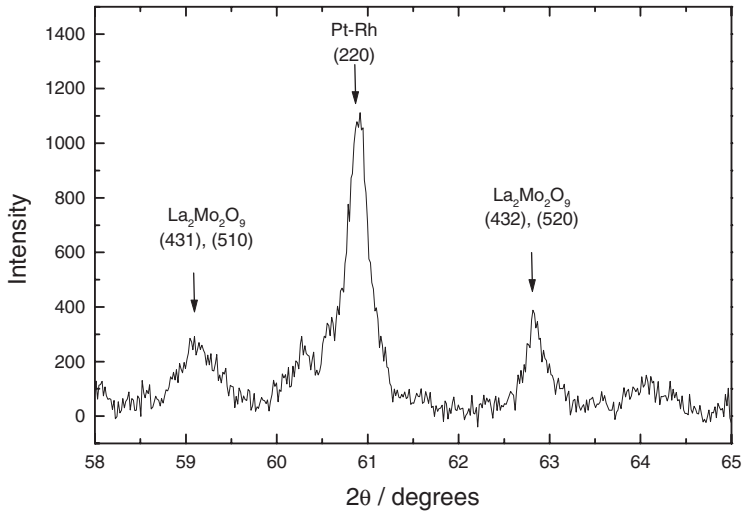

Figure 7. An enlargement of the diffraction pattern shown in figure 6 ($La_2Mo_2O_9$ on a Pt–Rh strip at 723 K) in the region near $2\theta = 60°$.

Figures 8(a) and (b) show the temperature dependence of the diffraction peaks around $2\theta = 61°$ (the Pt–Rh strip) and $2\theta = 59°$ ($La_2Mo_2O_9$). From figure 8(a), we can conclude that there are no sudden significant changes in the channel number to 2θ calibration function; the reduction in the diffraction angle is expected, as the sample undergoes thermal expansion. The typical deviation of the data from a simple straight line is of the order of three channels, or $0.05°$ of 2θ. Figure 8(b) indicates that the thermal behaviour of $La_2Mo_2O_9$ changes radically after its initial heating. During the first heating run, the behaviour of the phase transition appears to be second order, in agreement with the experiments described above, where the 2θ scale was determined precisely from the Si diffraction positions. However, subsequent runs show the transition to be first order, which was the behaviour observed by Goutenoire *et al* (2000). The transition temperature was not determined precisely, due to the inevitable scatter in these lattice parameter data. However, the transition can clearly be observed to lie between 823 and 873 K.

As a final test of the comparability of the calibrated and uncalibrated data sets, the approximate 2θ values for the (431), (510) peaks were used to determine approximate values of a as a function of temperature (figure 9). An error of $0.1°$ in 2θ is quite possible in the uncalibrated peak positions, and would lead to an error of approximately 0.01 Å in a. There is good agreement between the calibrated and uncalibrated results for the initial heating runs between room temperature and 1000 K. At even higher temperatures, the agreement is less good; it is not clear whether this is a real effect, reflecting changes in the $La_2Mo_2O_9$ sample due to a putative reaction with the Si standard or a change in the sample position altering the 2θ calibration.

The results of the neutron diffraction study of Goutenoire *et al* (2000) and the synchrotron x-ray study of Lacorre *et al* (2003) are also shown in figure 9, for comparison. The observed behaviours of the monoclinic phase vary substantially between the different experiments. There is also significant ambiguity in the thermal expansion of the cubic phase. The data of Lacorre *et al* (2003) give the lowest value of α, whilst the data of Goutenoire *et al* (2000) and the uncalibrated data in this study appear to agree rather well. The calibrated data presented in this study give a higher value of the thermal expansion coefficient, particularly above 1000 K.

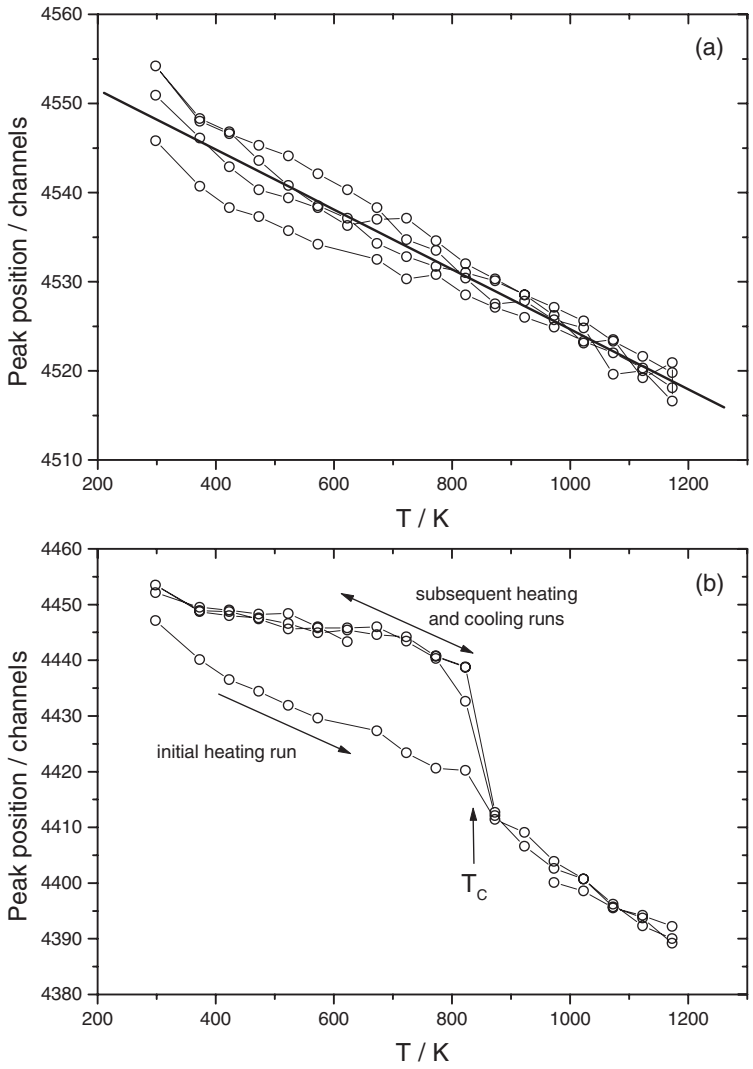

Figure 8. The temperature dependence of the positions of diffraction peaks for (a) the Pt–Rh sample strip and (b) $La_2Mo_2O_9$. The connecting lines between points show the order of the temperature runs. The heavy straight line in (a) fits all the data to a single straight line.

4. Discussion

Our experiments indicate that the transition between the non-conducting and conducting states in $La_2Mo_2O_9$ follows one of two distinct types of behaviour, though with a similar transition temperature. Where the material is quenched after synthesis, the phase transition to the high temperature conducting state is second order. However, subsequent slow cooling and re-heating of the sample results in a first-order transition. Whilst the character of the phase transition and the structural evolution below the transition are affected by these changes, the transition temperature appears to be relatively insensitive to these differences.

There is presumably some structural difference between the as-quenched and more slowly cooled lanthanum molybdate causing these changes. Any discussion of what that difference is

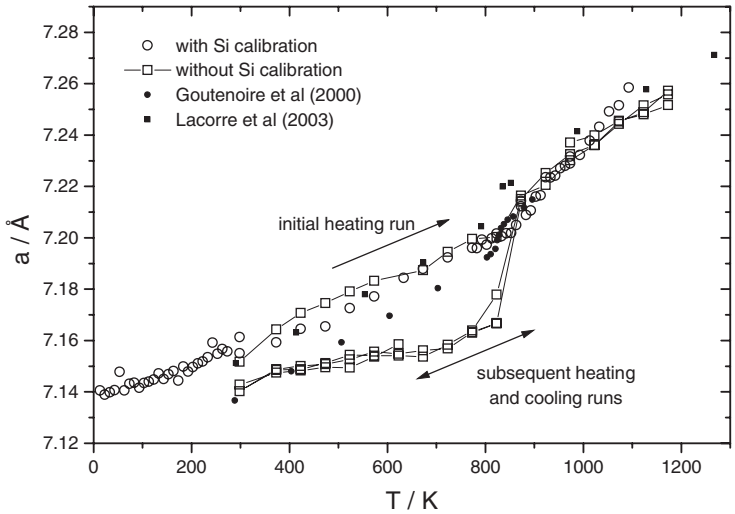

Figure 9. The temperature dependence of the pseudocubic lattice parameter a in $La_2Mo_2O_9$, measured while heating a fresh $La_2Mo_2O_9$ sample with Si calibrant (open circles) and while heating a fresh $La_2Mo_2O_9$ sample with no calibrant (open squares, joined by a line to show the order in which measurements were made). The results of the neutron diffraction study by Goutenoire *et al* (2000) and the synchrotron x-ray study by Lacorre *et al* (2003) are included for comparison.

will be rather speculative, given the difficulty of determining the complete crystal structure of $La_2Mo_2O_9$. However, the most plausible mechanism involves the ordering of oxygen. In the high temperature phase, the oxygen ions are mobile, and therefore dynamically disordered. If a sample of $La_2Mo_2O_9$ is cooled quickly enough, this dynamic disorder will be replaced by static disorder, analogous to the formation of a glass. Slow (equilibrium) cooling will allow the pattern of occupied oxygen sites to adopt an ordered array. Our results then imply that the transition between static and dynamic O disorder is second order, while the transition between dynamic disorder and static order is first order.

The precise evolution of the monoclinic phase with temperature will depend both on the degree of O order quenched into the system from high temperature, and on whether or not the degree of O order varies with temperature. Thus, the structural behaviour of the monoclinic phase will vary greatly with the thermal history of the sample. The same mechanism is likely to underpin the differences between our results (where the count time for each spectrum was of the order of 2 h, resulting in prolonged equilibration at high temperatures) and the experiments performed by Goutenoire *et al* (2000), who collected each diffraction pattern for approximately 5 min. These experiments, as summarized in figure 9, show that the evolution of the structure of the monoclinic phase of $La_2Mo_2O_9$ with temperature depends on the thermal history of the sample. This variability appears to be an intrinsic feature of the behaviour of $La_2Mo_2O_9$. However, the behaviours of different samples of $La_2Mo_2O_9$ in the cubic phase do not appear to show the same variation.

The response of the as-quenched $La_2Mo_2O_9$ to changes in temperature can be analysed as a second-order displacive phase transition, in the framework of Landau theory. From these measurements of the lattice parameters of $La_2Mo_2O_9$ as a function of temperature, we have identified two degrees of saturation at low temperature. Both of these are characterized by a temperature related to the temperatures below which changes with further cooling cease. The order parameter is essentially constant below $\theta_S/2$ and the baseline thermal expansion below $\theta_E/4$.

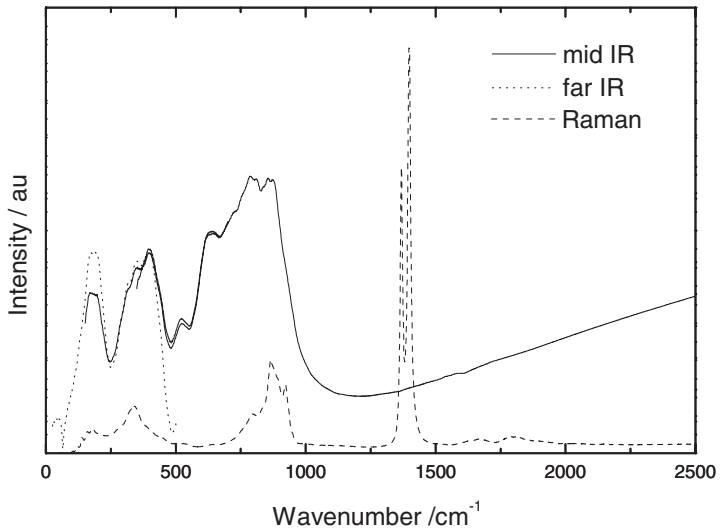

Figure 10. Infrared and Raman spectra of $La_2Mo_2O_9$ at room temperature. The relative intensities of the IR and Raman spectra are arbitrary.

Both the fitted saturation temperatures ($\theta_S = 165$ K, $\theta_E = 310$ K) can be converted to phonon frequencies. The Einstein temperature gives the Einstein frequency, which is some sort of 'average' frequency for the entire phonon distribution. The Einstein frequency, $\nu_E = k_B\theta_E/h$, for $La_2Mo_2O_9$ is 6.45 THz, or 215 cm^{-1}. Comparison with the room temperature Raman and IR spectra in figure 10 seems to imply that this is rather low, though this analysis depends a lot on which modes are actually IR and Raman active, and the number of modes present in the low frequency part of the spectrum. Precise identification of vibrational modes is difficult, since the unit cell of the room temperature structure is so large, and only slightly distorted from an ideal cubic structure.

Where the saturation of the order parameter is dominated by the saturation of a single mode, the mode frequency ν_S is related to the saturation temperature by $\nu_S = 2k_B\theta_S/h$ (Pérez-Mato and Salje 2001). For $\theta_S = 165$ K, this implies $\nu_S = 6.75$ THz $= 225$ cm^{-1}. This is in the range of the lowest frequency cluster of modes in the vibrational spectra, which is reasonable.

The possibility of making the phase transition in lanthanum molybdate second order has implications for the possible use of $La_2Mo_2O_9$ in devices, particularly if it becomes possible to use relatively large single crystals, rather than ceramics. The step change in the crystal structure at the transition temperature will cause internal stresses, particularly in large crystals, as the material is heated or cooled through the transition temperature, which are likely to lead to the crystal undergoing self-cataclasm (that is, breaking up due to stresses associated with the volume change) after repeated cycling. If the transition is second order, the structural changes are continuous and therefore potentially less damaging.

References

Born M and Huang K 1954 *Dynamical Theory of Crystal Lattices* (Oxford: Clarendon)

Carpenter M A, Salje E K H and Graeme-Barber A 1998 Spontaneous strain as a determinant of thermodynamic properties for phase transitions in minerals *Eur. J. Mineral.* **10** 621–92

Collado J A, Aranda M A G, Cabeza A, Olivera-Pastor P and Burque S 2002 Synthesis, structures and thermal expansion of the $La_2W_{2-x}Mo_xO_9$ series *J. Solid State Chem.* **167** 80–5

Faraday M 1839 *Experimental Researches in Electricity* (London: Taylor and Francis)

Georges S, Goutenoire F, Altorfer F, Sheptyakov D, Fauth F, Suard E and Lacorre P 2003 Thermal, structural and transport properties of the fast oxide-ion conductors $La_{2-x}R_xMo_2O_9$ (R = Nd, Gd, Y) *Solid State Ion.* **161** 231–41

Goutenoire F, Isnard O, Retoux R and Lacorre P 2000 Crystal structure of $La_2Mo_2O_9$, a new fast oxide-ion conductor *Chem. Mater.* **12** 2575–80

Goutenoire F, Isnard O, Suard E, Bohnke O, Laligant Y, Retoux R and Lacorre P 2001 Structural and transport characteristics of the LAMOX family of fast oxide-ion conductors, based on the lanthanum molybdenum oxide $La_2Mo_2O_9$ *J. Mater. Chem.* **11** 119–24

Hayward S A, Redfern S A T and Salje E K H 2002 Order parameter saturation in $LaAlO_3$ *J. Phys.: Condens. Matter* **14** 10131–44

Lacorre P, Goutenoire F, Altorfer F, Sheptyakov D, Fauth F and Suard E 2003 Crystal structure of new fast oxide-ion conductor $La_2Mo_2O_9$ *Adv. Sci. Technol.* **33** 737–47

Lacorre P, Goutenoire F, Bohnke O, Retoux R and Laligant Y 2000 Designing fast oxide-ion conductors based on $La_2Mo_2O_9$ *Nature* **404** 856–8

Pérez-Mato J M and Salje E K H 2001 Order parameter saturation at low temperatures: displacive phase transitions with coupled Einstein oscillators *Phil. Mag. Lett.* **81** 885–91

Salje E K H, Graeme-Barber A, Carpenter M A and Bismayer U 1993 Lattice parameters, spontaneous strain and phase transitions in $Pb_3(PO_4)_2$ *Acta Crystallogr.* B **49** 387–92

Wang X P and Fang Q F 2001 Low-frequency internal friction study of oxide-ion conductor $La_2Mo_2O_9$ *J. Phys.: Condens. Matter* **13** 1641–51

Wang X P and Fang Q F 2002 Effects of Ca doping on the oxygen ion diffusion and phase transition in oxide ion conductor $La_2Mo_2O_9$ *Solid State Ion.* **146** 185–93

Wang X P, Fang Q F, Li Z S, Zhang G G and Yi Z G 2002 Dielectric relaxation studies of Bi-doping effects on the oxygen-ion diffusion in $La_{2-x}Bi_xMo_2O_9$ oxide-ion conductors *Appl. Phys. Lett.* **81** 3434–6